Broadband Diffusing Wave Spectroscopy reveals microstructuring of polymer-drug system

*Sandra Jankovic, Simone Aleandri, Mathias Reufer, Martin Kuentz**

AUTHOR ADDRESS: *University of Applied Sciences and Arts Northwestern Switzerland, Institute of Pharma Technology, Muttenz, CH-4132 Switzerland*

KEYWORDS: macromolecular structuring, phase transition, broadband rheology, drug- polymer interaction

ABSTRACT

Microstructuring during a phase transition and crystallization in particular is critical for the physico-chemical properties of polymeric drug carriers and of the final dosage form. Extensive research has been dedicated to study polymeric matrices in drug delivery and despite of substantial progress, there are still unmet challenges such as a non-invasive mechanical analysis since classical rheological methods typically disturb the samples especially during a phase transition. This paper employs Diffusing Wave Spectroscopy (DWS) over a broad frequency band to study polymer-drug systems in a non-invasive way. Eutectic mixtures of polyethylene glycol (PEG) were investigated using two model drugs. While fenofibrate was barely interacting with the polymer, flurbiprofen provided a compound showing distinct molecular interactions with the carrier. Mechanical spectra were obtained during cooling of the molten polymer-drug systems. In conclusion, broadband DWS provided a better mechanistic understanding of the polymer-drug interactions and of macromolecular structuring during cooling of the eutectic melts. Such findings are relevant for a rationale design of pharmaceutical formulations during development and such knowledge would be also important for manufacturing to achieve drug products with reproducible quality characteristics.

INTRODUCTION

The rheological properties of pharmaceutically important materials such as polymer melts, colloids, gels, and dispersions are central to many fields of formulation development and manufacturing. Most mixtures exhibit complex rheological behavior since formulations include abundant polymers of different kinds.[1] Polymers that melt into a liquid are called to be thermoplastic and they are often processed by extrusion or molding. Polymeric crystallization may start when nuclei develop in a stochastic way and grow to a critical size in the cooling melt. Studies over the past two decades have provided important information on shear-induced crystallization and anisotropy in the direction of shear and show that crystallization proceeds as the nuclei grow into crystallites until all the melt has solidified.[2] When neighboring crystallites grow and segments of the chains forming these crystallites can no longer be incorporated into the crystalline domains, then amorphous regions start to form. This process is depending on the cooling rate so that a low cooling rate grants polymer chains more time to arrange or incorporate themselves into crystallites.[2]

Crystallization in synthetic polymers typically produces polycrystalline aggregates that are called spherulites given their spherical morphology. These spherulites are radially symmetric arrays of fibrillary crystallites ranging in diameter from less than one micron to several millimeters.[3] In pharmaceutical systems, previous research revealed that interactions between the polymer and a drug can influence the crystallization behavior of the polymeric matrix.[4] Indeed, molecular drug-polymer interaction can occur already in the molten state and may not be easily evidenced in the solid state.[5,6] Especially difficult is to study the crystallization process because such a phase transition is easily perturbed by the analytical method thereby leading to experimental bias.

Mechanical rheology has a long tradition in the study of polymer melts.[7] Shear stress controlled rheometers with high sensitivity allow measurement in the linear visco-elastic regime (LVR). Current rheological research on polymer crystallization attempts to combine the mechanical experiment with monitoring techniques such as nuclear magnetic resonance (NMR), small-angle X-ray scattering or dynamic optical microscopy.[8] However, any mechanical rheometry is not contact-free and it can be problematic to measure within the LVR when very dynamic changes occur such as during polymer crystallization. Shear stress controlled oscillatory measurements are further limited because of a narrow range of accessible high frequencies (with a maximum of about 100 Hz) and most important for the herein system, by the flow induced crystallization.[9,10]

Modern microrheology based on Diffusing Wave Spectroscopy (DWS) has significantly extended the range of experimentally accessible frequencies and it is possible to measure non-ergodic samples such as gels and semi-crystalline materials in a non-invasive way.[11–13]DWS has been used previously in the field of Pharmaceutics to study self-emulsifying formulations, emulsions as well as solid drug dispersions.[14–18]

The present research explores, for the first time, the effects of crystallization in a pharmaceutical polymeric system using DWS. Two eutectic systems with polyethylene glycol (PEG) and fenofibrate or flurbiprofen were employed as models.[4,19] This polymer type is hydrophilic with a crystalline lattice structure and can form eutectic mixtures with an active pharmaceutical ingredient (API). Specific interactions between PEG and a drug can suppress the crystalline polymer lattice to some degree during cooling of the molten blend. The model mixtures were selected for their ability to either specifically interact with PEG (e.g. flurbiprofen) or as a model for which no specific interactions are known (e.g. fenofibrate).[4,20] A particular aim of this DWS

pioneer study in polymer crystallization was to obtain insights into structure formation of the solidifying molten matrices upon cooling. This is not only of interest from a formulation perspective but also regarding manufacturing such as by hot melt extrusion.

MATERIALS AND METHODS

Materials

Fenofibrate was purchased from AK Scientific (30023 Ahern Ave Union City CA,USA), while poly(ethylene glycol) 6000, PEG was obtained from Sigma Aldrich (Riedstr. 2 D89559 Steinheim 497329970). Flurbiprofen was supplied by Acros Organics (New Jersey USA) and uniform $Ti0_2$ particles were obtained from LS Instruments (Fribourg, Switzerland).

Methods

Preparation of the eutectic mixtures

Eutectic mixtures were prepared by using the melting method as described in literature.[21] Briefly, the PEG 6000 binary mixtures contained 24% (w/w) fenofibrate or alternatively 33% (w/w) of flurbiprofen. These concentrations were obtained from previous DSC measurements, (i.e. as mixtures with one endothermic event) as reported in literature.[4] The physical mixture was blended with a spatula in a metallic pan and heated up to 90°C in order to assure complete melting. The heat exposure during preparation and analysis of the eutectic mixtures was not expected to cause any drug degradation of the two rather stable compounds in line with previous reports that employed hot melt extrusion.[22,23] The obtained molten mixture in the present work was then cooled

down to room temperature and kept in a desiccator before analysis. Characteristics and compositions for various drug-PEG eutectic systems are described in **Table 1.**

Powder x-ray diffraction (XRPD)

Powder X-ray diffraction was used to characterize the solid form of the physical mixtures and of solid dispersions at ambient temperature using a Bruker D2 PHASER (Bruker AXS GmbH, Germany) with a PSD-50 M detector and EVA application software version 6. Samples were prepared by spreading powder samples on PMMA specimen holder rings from Bruker. Measurements were performed at 25°C with a Cu Kα radiation source at 30 kV voltage, 10 mA current and were scanned from 6-40 2θ, with 2θ being the scattering angle at a scanning speed of 2 °/min.

Differential scanning calorimetry (DSC)

A DSC 3 system (Mettler Toledo, Greifensee, Switzerland) was calibrated for temperature and enthalpy using indium. Nitrogen was used as the protective gas (200 mL/min). Samples (approximately 5 mg) were placed in 40 µL aluminium pans with pierced aluminium lids. The melting point (T_m) was determined by a single-segment heating ramp of 10 °C/min from 25 °C to a maximum temperature of 200 °C. All DSC measurements were carried out in triplicate.

Fourier transform infrared spectroscopy

Attenuated total reflection Fourier transform infrared (ATR-FTIR) spectra of pure compounds and

SDs were acquired in the 4000–600 cm^{-1} range using a Cary 680 Series FTIR spectrometer (Agilent Technologies, Santa Clara, USA) equipped with an attenuated total reflectance accessory. A scanning range of 4000–600 cm was selected with 42 scans and a resolution of 4 cm. The spectra were evaluated using the software ACD/Spectrus Processor 2016.1.1 (Advanced Chemistry Development Toronto, Canada).

Diffusing wave spectroscopy (DWS)

Measuring principle: DWS is a light scattering technique that requires turbid samples to study the dynamic properties. In the transmission geometry, the sample is illuminated by a expanded laser light source and the transmitted light is analyzed on the opposite side.[24] The colloidal scattering particles can be present inside the sample, such for example oil droplets in emulsion, or they can be added in case of transparent sample such as, for example by dispersing titanium dioxide. Light detectors measure the intensity of the scattered light. The fluctuations of scattered light are characterized by the normalized intensity autocorrelation function (eq.1)[24]

$$g_{(2)}(t)=\langle I(t_0)I(t_0+t)\rangle/\langle I\rangle^2 \quad (1)$$

where the quantity $\langle I\rangle$ is the average intensity, while t represents the lag time.

Using the Siegert relation (eq.2), the intensity correlation function and the field autocorrelation are related:

$$g_{(2)}(t)=1+\beta|g_{(1)}(t)|^2 \quad (2)$$

where β is an instrumental factor given by the collection optics. Once the field correlation function and l^* have been measured, the mean square displacement (MSD, $\langle \Delta r^2(t) \rangle$) of a sample can be calculated employing (eq.3)[10,25]:

$$g_{(2)}(t)\text{-}1 \propto \left| \int_0^\infty P(s) exp\left[-\frac{1}{3} k^2 < \Delta r^2(t) > \frac{s}{l^*} \right] ds \right|^2 \quad (3)$$

where $k = 2\pi n/\lambda$ is the optical wavenumber including n as the refractive index of the medium and λ is the laser wavelength. $P(s)$ represents the distribution of the photon trajectories of length s in the sample of thickness L, while l^* is the transport mean free path which characterizes the typical step length of the photon random walk.

The data obtained for the MSD were analyzed employing the function proposed by Bellour and coworkers[26]:

$$< \Delta r^2(t) >= 6\delta^2 \left(1 - e^{-\left(\frac{D_0}{\delta^2} t\right)^\alpha} \right)^{1/\alpha} \left(1 + \frac{D_m}{\delta^2} t \right) \quad (4)$$

Where δ^2 represents the amplitude of particle motion, t is the lag time, D_o and D_m are the short and long time diffusion coefficient while α is an additional parameter introduced to take into account the broad spectrum of relaxation times at the plateau onset time.

Eq. 4 has been recently extended to better describe the region of longer relaxation times in case of pharmaceutical emulsions. [27] On the other hand eq. 4 can also be simplified for other systems. Bellour et al. suggested the following eq. 5 for particles that are harmonically bound (i.e. "entrapped") to exhibit Brownian motion around a stationary mean position:

$$< \Delta r^2(t) >= 6\delta^2 \left(1 - e^{\frac{-D_0}{\delta^2}t}\right) \quad (5)$$

It is here possible to approximate the displacement value of the plateau with $6\delta^2$. The present work determined this plateau value based on the obtained MSD at the estimated inflection point.

Experimental setup: All samples were measured in transmission mode using a DWS RheoLab instrument (LS Instruments AG, Fribourg, Switzerland). The theory of DWS-based microrheology was already explained in detail in our previous work.[16] In brief, the laser light was scattered from the ground glass and collimated by a single lens before illuminating the sample. To avoid time consuming measurements at low frequencies, the instruments uses the so-called echo technique. The echo completes the data set to obtain the ICF over a broad range of lag times. In the echo mode the ground glass rotates during the measurement producing different illumination speckle pattern.[15] This feature is particularly important when working with non-ergodic samples, such as emulsions, gels and semi-crystalline polymers.[15,16] Samples were analyzed using a 5mm thickness cuvette. To ensure turbidity of the molten polymer and of the solid dispersion, 4.5 mg of titanium dioxide tracer particles with mean diameter of 360 nm were added and mixed with 2 g of sample. The mixture was poured into the cuvette to fill it up to 15-20 mm. The measurements were set in slow rotation mode at 300s with 30 s of echo mode. Five measurements of each temperature were done with two independent samples. The average of ten measurements is presented in all graphs.

Hot stage cross polarized microscopy

An assessment of the crystal nucleation and growth was based on polarized light imaging using a heating stage coupled with a microscope Axioskop 2 mot (upright). The latter had a Hamamatsu

5810 3CCD video camera and was equipped with phase contrast, polarized filters, and DIC. Physical mixtures were molten at 85° degrees and the crystallization was studied using a remained constant magnification throughout the whole measurement (scale bars are displayed in every image).

Molecular visualization by docking

To qualitatively analyze and depict drug interactions with the polymer, molecular docking was conducted. Chemical structures were obtained from the ChemicaElectrica Gateway (v. 4.01) and loaded into Molecular Modeling Pro Plus (v.8.2.1.) (both programs by Norgwyn Montgomery Software Inc., North Wales, USA). A relatively shorter chain for polyethylene glycol (i.e. PEG 400) was selected as model and this structure was drawn together with either the drug fenofibrate or flurbiprofen. Following a molecular mechanics minimization of the conformational energy (using the MM2 algorithm), partial charges of the molecules were calculated based on a semi-empirical quantum mechanical method (using a Complete Neglect of Differential Overlap, CNDO approach). Starting from 6 Angstroms distance between the molecular Van der Waals surfaces, a grid search algorithm proposed a molecular docking configuration of minimized energy. A relative permittivity of 18 was selected to approximate the PEG environment.[28]The final molecular association was depicted as combined wire frame and space filled model.

RESULTS

Solid state characterizations

Raw materials and the eutectic mixtures of PEG 6000 with either fenofibrate or flurbiprofen were characterized initially. Solid state analysis such as by DSC, PXRD and FT-IR was performed to determine the physical state of the raw materials and of the eutectic mixtures as well as to study interactions in both the molten and solid state.

While the composition of eutectic mixtures and the respective melting point are presented in **Table 1**, the molecular docking of the two compounds with the carrier employed is presented in **Fig. 1.** The DSC thermograms of pure PEG 6000, fenofibrate and flurbiprofen, as well as of their eutectic mixture are shown in **Fig. 2A**. The analysis of pure PEG 6000 shows that the onset of the endotherm occurs at 58 °C, having a peak at 62.5 °C. While the pure drug fenofibrate had a melting point of 80.2 °C and flurbiprofen's melting point was 114 °C, the endothermic event of the eutectics was much lower compared to the raw materials. The eutectic composition for PEG and fenofibrate has been determined previously to comprise 24% (w/w) of drug and it was independent of the molecular weight of the carrier.[29] Due to a strong hydrogen bonding, the eutectic composition for PEG and flurbiprofen was much higher with 33% (w/w) of API and strongly influenced by the molecular weight of the polymer. [4,19] As eutectic systems, the crystallinity of the pure drugs was affected in mixture regarding form as well as extent, thereby resulting in the observed DSC endotherms. The molecular interaction of the two model drugs with a PEG chain was also visualized based on molecular modeling (i.e. molecular docking of API to a polymer chain). **Fig. 1** depicts the hydrogen bond that is formed in the case of flurbiprofen whereas no such strong interaction was possible in case of fenofibrate with PEG.

The crystalline state of the raw materials and of the eutectics was analyzed further by PXRD. As observed in **Fig. 2B**, raw material and eutectics present distinct Bragg peaks, indicating a crystalline nature. When comparing the spectra of the raw flurbiprofen with that of the eutectic

mixture, a slight shift in the location of the peaks was observed. The interaction between flurbiprofen and PEG 6000 was further evaluated by FT-IR. Pronounced shifts in the absorption bands of FT-IR are visible in **Fig. 3** when comparing the spectra of flurbiprofen and fenofibrate as raw material and those obtained from the respective eutectic formulations**.** It can be seen that the carbonyl stretching band of flurbiprofen's carboxyl moiety at 1700 cm^{-1} band has shifted to a higher frequency in the eutectic mixture. It has been argued that flurbiprofen is able to both donate and accept hydrogen bonds via the carboxyl moiety depending on the molecular weight of the polymer.[4] It is likely that flurbiprofen is able to donate hydrogen bonds with PEG 6000, while it might also accept hydrogen bonds with much lower molecular weight PEG considering a more relevant influence of hydroxyl groups present at the chain ends.[30] This is according to the expected molecular interaction based on molecular docking (**Fig. 1**) and the previously reported changes in FT-IR spectroscopy in mixtures of flurbiprofen and PEG.[4,19] Such a shift was not observed in the case of the fenofibrate and the eutectic mixture of this drug. There were also not pronounced changes in the lower wave number vibrations in case of the pure fenofibrate compared to that of the eutectic mixture. This was again different for the system of flurbiprofen where at relatively lower wave numbers, some changes were observed in the spectra; especially a peak at 696.16 cm^{-1} that was shifted towards lower wavenumber (630.60 cm^{-1}) for the solid dispersion of flurbiprofen with PEG.

DWS

Analysis of polymer crystallization and macromolecular structuring was a central aim of this study. Recent progress in DWS allows measuring at changing temperatures in a dynamic way so that a solidification of eutectic melts with and without drug could be analyzed.

Fig. 4A presents the intensity correlation function (ICF) of PEG 6000 from 85 °C to 48 °C. At 85 °C when the polymer was completely molten, the intensity correlation function decayed to zero. Upon cooling, such decay occurred at longer lag time, and this abrupt shift was due to high viscosity increase that was expected by polymer nucleation and crystal growth since PEG 6000 is a semi-crystalline polymer at room temperature. The major changes in intensity correlation function were observed between 49 and 48 °C and the shift in lag time is displayed in **Fig. 4B**, where MSD is plotted. At relatively high temperature, the system was liquid and the MSD was linearly increasing with lag time, while with temperature decreased, the MSD was reaching a plateau. Such a plateau means that tracer particles exhibit limited Brownian motion as they become entrapped. Complex viscosity versus the frequency is presented in **Fig.4C.** While at high temperature, the polymer was behaving as a Newtonian system with constant viscosity across a broad range of frequencies, this was different at lower temperatures, for which viscosity was changing with frequency thereby suggesting a structuring in the course of polymer crystallization leading to shear thinning. Mean count rate (MCR) represents the average intensity of light (proportional to the number of photons arriving at the detector) that is an indicator of sample transparency. At the higher end of measured temperatures, MCR was around 300 kHz, whereas with the onset of polymer crystallization there was a strong decrease of the MCR, indicating an increase of turbidity. (**Fig. 4D)**. This provided a sensitive analytical approach to the macroscopic appearance of the polymer that was transparent at 85°C but white at room temperature. In PEG 6000 is a semi-crystalline polymer and the increase of turbidity was due to the crystallization of the polymer occurring around 48 °C.

The molten physical mixture of PEG 6000 and fenofibrate was then heated to 85 °C **Fig. 5A** compares the intensity correlation function (ICF) upon cooling to lower temperatures and 45.4°C

can be identified as the temperature of crystallization. Thus, at 85 °C when the polymer was completely molten, the ICF decayed to zero, whereas the ICF started to no longer reach zero upon cooling. ICFs were shifted to higher values of lag time(s) and the viscosity was increasing. The major changes in intensity correlation function for the eutectics were observed between 46 and 45.4 °C. The shift in lag time is depicted in **Fig. 5B**, where MSD is plotted versus lag time. At high temperature for which the system is liquid, the MSD was increasing linearly with lag time, while upon decreasing the temperature, the MSD was reaching a plateau. Changes of the complex viscosity versus temperature are presented in **Fig.5C.** Similar to pure PEG 6000, the molten polymer mixture had a constant viscosity over the measured frequency range, whereas at lower temperatures, there was a decrease of viscosity over the frequency range suggesting again shear thinning as previously observed with pure PEG 6000. Further analysis of the fenofibrate and PEG 6000 mixture is given by **Fig. 5D** that shows the decrease of the MCR over the temperature for this eutectic system. At higher temperatures, MCR was approximately 300 kHz and a strong decrease of the MCR, indicated an increase of turbidity in the course of matrix crystallization. The onset of crystallization was occurring at a temperature of about 45 °C and MCR reached approximately 220 kHz when the sample was completely solidified.

Finally, the model of the strongly interacting mixture was analyzed using PEG 6000 in combination with flurbiprofen. The molten mixture at 85 °C showed again an ICF that was decaying to zero. However, with a decrease of temperature there was again a shift to higher lag times, indicating a higher viscosity of the system as it can be seen in **Fig.6A.** For this eutectic mixture, no solidification was observed even close to the body temperature (38° C) in line with what has been reported before.[4] Again the MSD provided insights into the microstructure via the mean average distance that tracer particles were travelling. (**Fig. 6B**). In the liquid state, tracer

particle were able to perform Brownian motion and therefore, there was a linear increase of MSD versus lag time. For a nearly constant MSD, tracer particles were apparently confined around their mean positions. When considering **Fig 6C**, the systems does not exhibit an ideally viscous behavior at high temperature; therefore, an apparent shear thickening may have caused the observed frequency changes at 85°C, while cooling of the system was leading to a rheological behavior suggesting shear thinning similar to the previously analyzed samples. Such cooling led again to a strong decrease of MCR values due to the occurrence of crystallites as shown **Fig 6D.** Since all samples showed a plateau regime of MSD, a comparison for this apparent confinement of the tracer particles due to microstructuring of the solidifying polymer matrix. Following the approach of Bellour et al.[26] (Eq. 5) for the present case of polymeric melts, the given confinement of the tracer particles can be plotted as a kind of "cage size" as displayed in **Fig. 7**. The dimension of this apparent confinement of tracer particles was biggest for polymer alone, followed by the eutectic mixtures with fenofibrate and finally that with flurbiprofen. The data of DWS were finally complemented by studies using hot stage cross polarized microscopy and the results are presented in **Fig.8A, B and C** respectively. As mentioned before, polymer drug interaction play a significant role in polymer chain folding during the crystallization and as highlighted in the **Fig. 8C,** the crystalline structure of the SD with flurbiprofen in the solid state appeared to be different compared to the polymer alone or also compared to the SD with fenofibrate that was less interacting with the polymer matrix. It is evident that the crystalline structure was in the latter case rather disrupted in line with previous reports in the literature.[5,19,29]

DISCUSSION

Crystallization of polymers is a complex topic and the classical of Hoffmann-Lauritzen theory provides a basic understanding of how polymeric chains exhibit surface crystallization into lamellae of a given thickness.[31] Since these pioneer days, several more refined theoretical models involving multistep crystallization have been proposed and a very recent review in the journal Macromolecules comes to the conclusion that even these days, important theoretical questions remain unanswered.[32] The theoretical complexity is of course even increased in presence of additives such as a drug and therefore, pharmaceutical research has mostly taken just a phenomenological approach to crystallization of polymeric drug formulations. However, any experimental study of a phase transition such as crystallization is also difficult because the analytics should not disturb the observed process, which is a concern with techniques such as mechanical rheology. The present work therefore used for the first time broadband DWS to study pharmaceutical eutectic model systems in the course of solidification upon cooling.

Previous work suggested that flurbiprofen is strongly interacting with PEG while fenofibrate is not.[4] Solid state characterization employing DSC, PXRD were performed and the results are shown in **Fig. 2**. Specific interactions such as hydrogen bonding between flurbiprofen and PEG 6000 have been studied with FT-IR and presented in **Fig 3.** The current study found that drug-polymer interaction played a key role in case of flurbiprofen during phase transition of the PEG-based solid dispersion. It can be well imagined that strongly attached flurbiprofen would affect polymer chain flexibility and its bulkiness so that crystalline packing of lamellae would be affected. This qualitative view may explain the observed effects on polymer matrix crystallization in case of this strongly interacting eutectic system. The solid dispersion comprising PEG 6000 and fenofibrate exhibited ideal viscous behavior at high temperatures and the frequency spectrum suggested some

viscoelastic behavior at lower temperatures. (**Fig. 4C** and **5C**). The high temperature regime can be imagined to hold for a typical melt with polymer chains that can arrange in random coils and thereby provide a rather homogenous system with practically ideal viscous behavior. Once polymer nucleation and growth occurs, the lamellar grow into crystallites and such spherulites can further aggregate. Since these aggregates provide suspended particles, there was turbidity noted as indicated by the MCR of the DWS experiments. The frequency dependence of viscosity was analogues to shear thinning of a suspension and a recent study actually evaluated typical models of suspension rheology for such samples.[33]The authors pointed to the analogy of particle hierarchy between aggregated crystallites and other polymeric nanocomposites. The latter nanocomposites are typically agglomerates of small aggregates and these again consist of primary nanoparticles. Analogously, crystal aggregates (spherulites) are aggregates of crystal lamellae consisting of several individual lamellae.

Aggregated polymeric crystals can exhibit mechanical rigidity and therefore elastic behavior. Determination of the solidification point is obtained using the crossover point of *G'* and *G''* and the results presented in **Table 2**. Indeed, above the given crystallization temperature, samples were in molten state exhibiting *G''* > *G'*, while upon solidification, there was dominance of the elastic modulus with *G*' > *G''*. (data not shown)

Newtonian behavior at high temperatures was not found in case of the molten solid dispersion with flurbiprofen. (**Fig. 6C**) The changes along the differences frequencies suggested increasing viscosity at 85 °C, whereas upon cooling, data indicated again a shear thinning behavior. The latter behavior supports the view that occurrence of crystallites was leading to a suspension-type of rheology. However, the behavior at 85°C in the melt is particularly notable since PEG 6000 alone

365 did not show such increased viscosity with frequency but was rather Newtonian. Polymers of
366 higher molecular weight can show an increase of viscosity with rising frequency which is due to
367 the entanglement of longer chains. Each detanglement is expected to require a specific relaxation
368 time and for higher frequencies, transient bonds of entanglement would become permanent on the
369 given time scale.[34] Even though a strongly interacting small-molecular drug like flurbiprofen
370 would not greatly lengthen the chains of PEG 6000, the present results still display some frequency
371 dependency of the viscous melt caused by the presence of flurbiprofen.

372 The presence of strong molecular interactions between a drug and PEG 6000 was also studied by
373 Van Duong et al. (2017). They outlined the view that in the melt, PEG chains are locked in
374 hydrogen bonding with drug molecules and therefore no more than one repeated unit of helical
375 structure can be folded. The crystallization process for the considered systems is taking place in a
376 relatively narrow temperature range, and this may occur especially when the system is
377 homogeneously dispersed. The model assumes that in the course of chain folding, drug-polymer
378 hydrogen bonds are disrupted leading to a segregation of API. Some drug remains hydrogen
379 bonded to the surface of the folded lamellae and is part of drug-rich domains. Such solidified
380 polymer systems are typically semi-crystalline and the extent of crystallinity as well as the given
381 microstructure were previously mentioned to likely affect quality attributes such as drug release
382 .[4,5]

383 To gain a better understanding of how the presence of drug affected polymer crystallization, the
384 average movement of the tracer particles as MSD grants insights into the microstructuring in the
385 course of crystallization. The approach by Bellour et al. [26] has been previously used to describe
386 other structured liquids such as a surfactant solution of worm-like micelles and it was qualitatively
387 used in the present study to interpret the obtained data of the polymeric melts upon

crystallization.[26] When tracer particles exhibit a nearly constant MSD for a regime of frequencies (or lag times), then there is a kind of apparent entrapment given. The so-called "cage size" grants indirect insights into the structure of the matrix that is surrounding the used tracer particles. It is noteworthy that the MSD decreases in presence of polymer drug interaction, which is also reflecting by the apparent cage size at the inflexion point (named as $6\delta^2$) as presented in **Fig.7**. Given that tracer particles were embedded in a matrix of crystallizing and aggregating lamellae, the differences in apparent cage size may suggest how finely meshed these networks of lamellae were. This would support the view that the strongly interacting flurbiprofen perturbs polymer crystallization thereby leading to relatively smaller lamellae compared with pure PEG 6000 or its SD with fenofibrate. Indeed, the presence of flurbiprofen attached to the PEG via hydrogen bonding would inhibit the crystallization of the polymer, because it induces defects in the PEG crystalline network, hindering it from growing and structuring in line with results depicted in **Fig.8**. The present findings show that microstructuring of polymer in presence of drug can be studied not only by small-angle X scattering but also with novel microrheological tool such as broadband DWS.[35,36]

These findings help us to understand the microstructuring during phase transition of the polymer and of eutectic mixtures at high frequencies and in a non-invasive conditions. In addition, physicochemical properties and pharmaceutical performance of PEG-based solid dispersion depend on the drug-polymer interactions. Disruption of the crystalline lattice has also expected implications of drug release in that a relatively lower matrix crystallinity typically shows faster drug release compared to an eutectic system with a higher degree of crystallization. Therefore, the given microstructure is central for the quality attributes of the given SD formulations and present

work may find applications in formulation development as well as in process development of a eutectic drug product.

CONCLUSIONS

The physico-chemical properties of polymeric drug carriers and of the final dosage form depend on the microstructuring during the crystallization process in case of polymer eutectics. DWS and MSD were employed to study macromolecular structuring during cooling of the PEG-based mixtures with two model drugs, fenofibrate and flurbiprofen. While the first compound was barely interacting with the polymer, flurbiprofen provided a distinct molecular interaction with the carrier. This interaction already present in the molten state was changing the rheological behavior of the otherwise pure polymer melt. The crystallization of polymer was monitored by studying complex viscosity and MSD parameters from DWS. Indirectly it was possible to gain insights into how lamellae may crystalize and aggregate in the different formulations. Given the importance of the microstructure of such eutectic systems on different pharmaceutical quality attributes, the present findings are of high relevance also for practical formulation development. Compared to classical rheological measurements where the directions of the crystallizing lamellae are influenced during the measurements, DWS offers insights into the microstructuring of crystallizing lamellae based on contact-free measurements over a broad frequency range. Such mechanistic analysis and understanding of microstructuring under non-invasive conditions is not only relevant for eutectic systems. Other solid drug dispersions could be studied in the future too and tracer particles should be added whenever a system does not provide sufficient light scattering on its own. Therefore, DWS is a quite versatile tool to study the solidification behavior of drug-excipient

mixtures, which is important to properly understand phase behavior and microstructuring of pharmaceutical formulations.

TOC

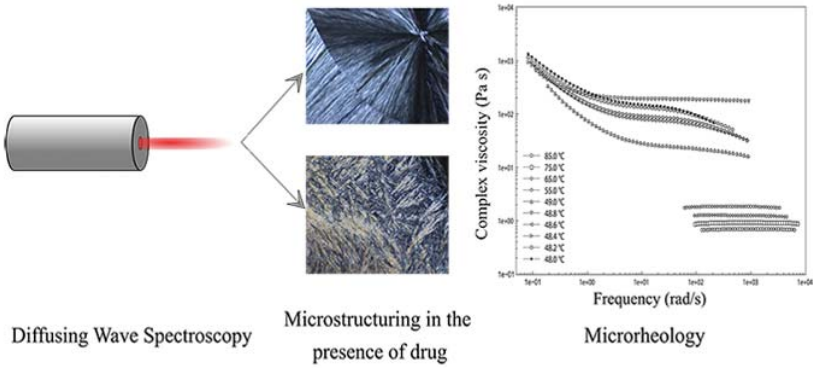

This paper employs Diffusing Wave Spectroscopy (DWS) over a broad frequency band to study polymer-drug systems in a non-invasive way. Eutectic mixtures of polyethylene glycol (PEG) were investigated using two model drugs: fenofibrate and flurbiprofen. While the first model compound was barely interacting with the polymer, flurbiprofen showed pronounced molecular interaction with the polymer, thereby influencing the microstructuring of the system.

FIGURES

Fig. 1. Molecular docking of PEG 6000 with fenofibrate (A) and flurbiprofen (B)

Fig. 2. Differential Scanning Calorimetry (DSC) (A) and Powder X-ray diffraction (XRPD) (B) plots of fenofibrate (a), flurbiprofen (b), PEG c) PEG –fenofibrate SD (d) and PEG- flurbiprofen SD (e).

Fig. 3. FT-IR of flurbiprofen (gray solid line), solid dispersion with flurbiprofen (gray dots), fenofibrate (black solid line), solid dispersion with fenofibrate (black dots).

Fig. 4. Microrheological characterization of PEG 6000: ICF (A), MSD (B), complex viscosity (C) and MCR (D).

Fig. 5. Microrheological characterization of solid dispersion of PEG 6000 and fenofibrate: ICF (A), MSD (B), complex viscosity (C) and MCR (D).

Fig. 6. Microrheological characterization of solid dispersion of PEG 6000 and flurbiprofen: ICF (A), MSD (B), complex viscosity (C) and MCR (D).

Fig. 7. Comparison of the apparent cage size (named as 6□ 2) in pure PEG, SD of fenofibrate and SD of flurbiprofen close to their solidification temperature.

Fig. 8. Hot stage cross polarized light microscopy of PEG 6000 (A), SD of fenofibrate (B) and SD of flurbiprofen (C)

TABLES

Table 1. Characteristics and composition for various Drug-PEG eutectic systems

Compound	Molecular weight (MW)	T_m (°C)	ΔH_f (kJ/mole)	Molar volume (cm^3/mol)	cLog*P* (n-octanol/water)	Experimental eutectic composition with PEG 6000 (%)	References
Fenofibrate	361	80.2	34.0	310.7	4.43	24	[20]
Flurbiprofen	244	114.7	28.0	263.5	4.12	33	[19]
PEG	6000	58-63	-	-	-	-	

Table 2. Temperatures and *G' G'* values at the intersection of curves

	Temperature (°C)	Frequency (rad/s)	Moduli *G' G''* (Pa)
PEG	48.20 48.00	0.63 0.70	120.00 150.60
SD of fenofibrate	45.60 45.40	2.69 0.50	19.54 398.58
SD of flurbiprofen	38.40 38.20	0.12 1.64	151.40 1958.76

AUTHOR INFORMATION

Corresponding Author

Martin Kuentz - *University of Applied Sciences and Arts Northwestern Switzerland, Institute of Pharma Technology, Muttenz, CH-4132 Switzerland*, E-mail: martin.kuentz@fhnw.ch

Authors

Sandra Jankovic - *University of Applied Sciences and Arts Northwestern Switzerland, Institute of Pharma Technology, Muttenz, CH-4132 Switzerland;University of Basel, Department of Pharmaceutical Sciences, Basel, Switzerland*

Simone Aleandri - *University of Bern, Department of Chemistry and Biochemistry, Bern, Switzerland*

Mathias Reufer - *Zumbach Electronic, Hauptstrasse 93, Postfach, 2552 Orpund, Switzerland*

ACKNOWLEDGMENT

This project has received funding from the European Union's Horizon 2020 Research and Innovation Programme under grant agreement No 674909 (PEARRL). We are grateful to Prof. Dr. Mezzenga for the use of the hot stage cross polarized microscopy at ETH and Theodor Bühler for the assistant in FT-IR measurements. We further thank Prof. Frank Scheffold for his valuable comments in the preparation of the manuscript.

REFERENCES

(1) Matsen, M. W. Soft Matter, Volume 1: Polymer Melts and Mixtures. Wiley-VCH Weinheim 2006.

(2) Singh, Y. Martin's Physical Pharmacy and Pharmaceutical Sciences. *Rutgers, State Univ. New Jersey* **2006**.

(3) Martin, A.; Swarbrick, J.; Cammarata, A. Physical Pharmacy. *Lea Febiger* **2006**.

(4) Vippagunta, S. R.; Wang, Z.; Hornung, S.; Krill, S. L. Factors Affecting the Formation of Eutectic Solid Dispersions and Their Dissolution Behavior. *J. Pharm. Sci.* **2007**, *96* (2), 294–304. https://doi.org/10.1002/jps.20754.

(5) Van Duong, T.; Reekmans, G.; Venkatesham, A.; Van Aerschot, A.; Adriaensens, P.; Van Humbeeck, J.; Van den Mooter, G. Spectroscopic Investigation of the Formation and Disruption of Hydrogen Bonds in Pharmaceutical Semicrystalline Dispersions. *Mol. Pharm.* **2017**, *14* (5), 1726–1741. https://doi.org/10.1021/acs.molpharmaceut.6b01172.

(6) Broman, E.; Khoo, C.; Taylor, L. S. A Comparison of Alternative Polymer Excipients and Processing Methods for Making Solid Dispersions of a Poorly Water Soluble Drug. *Int. J. Pharm.* **2001**, *222* (1), 139–151. https://doi.org/10.1016/S0378-5173(01)00709-8.

(7) De Kee, D.; Wissbrun, K. F. Polymer Rheology. *Phys. Today* **1998**, *51* (6), 24–29. https://doi.org/10.1063/1.882283.

(8) Räntzsch, V.; Özen, M. B.; Ratzsch, K.; Stellamanns, E.; Sprung, M.; Guthausen, G.; Wilhelm, M. Polymer Crystallization Studied by Hyphenated Rheology Techniques: Rheo-NMR, Rheo-SAXS, and Rheo-Microscopy. *Macromol. Mater. Eng.* **2019**, *304* (2), 1800586. https://doi.org/10.1002/mame.201800586.

(9) Del Giudice, F.; Tassieri, M.; Oelschlaeger, C.; Shen, A. Q. When Microrheology, Bulk Rheology, and Microfluidics Meet: Broadband Rheology of Hydroxyethyl Cellulose Water Solutions. *Macromolecules* **2017**, *50* (7), 2951–2963. https://doi.org/10.1021/acs.macromol.6b02727.

(10) Dasgupta, B. R.; Tee, S.-Y.; Crocker, J. C.; Frisken, B. J.; Weitz, D. A. Microrheology of Polyethylene Oxide Using Diffusing Wave Spectroscopy and Single Scattering. *Phys. Rev. E* **2002**, *65* (5), 051505. https://doi.org/10.1103/PhysRevE.65.051505.

(11) Pine, D. J.; Weitz, D. A.; Zhu, J. X.; Herbolzheimer, E. Diffusing-Wave Spectroscopy: Dynamic Light Scattering in the Multiple Scattering Limit. *J. Phys.* **1990**, *51* (18), 2101–2127. https://doi.org/10.1051/jphys:0199000510180210100.

(12) MacKintosh, F. C.; John, S. Diffusing-Wave Spectroscopy and Multiple Scattering of Light in Correlated Random Media. *Phys. Rev. B* **1989**, *40* (4), 2383–2406. https://doi.org/10.1103/PhysRevB.40.2383.

(13) Pine, D. J.; Weitz, D. A.; Chaikin, P. M.; Herbolzheimer, E. Diffusing Wave Spectroscopy. *Phys. Rev. Lett.* **1988**, *60* (12), 1134–1137. https://doi.org/10.1103/PhysRevLett.60.1134.

(14) Jankovic, S.; O'Dwyer, P. J.; Box, K. J.; Imanidis, G.; Reppas, C.; Kuentz, M. Biphasic Drug Release Testing Coupled with Diffusing Wave Spectroscopy for Mechanistic Understanding of Solid Dispersion Performance. *Eur. J. Pharm. Sci.* **2019**, *137*, 105001. https://doi.org/10.1016/j.ejps.2019.105001.

(15) Reufer, M.; Machado, A. H. E.; Niederquell, A.; Bohnenblust, K.; Müller, B.; Völker, A. C.; Kuentz, M. Introducing Diffusing Wave Spectroscopy as a Process Analytical Tool for Pharmaceutical Emulsion Manufacturing. *J. Pharm. Sci.* **2014**, *103* (12), 3902–3913. https://doi.org/10.1002/jps.24197.

(16) Niederquell, A.; Völker, A. C.; Kuentz, M. Introduction of Diffusing Wave Spectroscopy to Study Self-Emulsifying Drug Delivery Systems with Respect to Liquid Filling of Capsules. *Int. J. Pharm.* **2012**, *426* (1–2), 144–152. https://doi.org/10.1016/j.ijpharm.2012.01.042.

(17) Alexander M, Piska I, D. D. Investigation of Particle Dynamics in Gels Involving Casein Micelles: A Diffusing Wave Spectroscopy and Rheology Approach. *Food Hydrocoll.* **2008**, *22* (6), 1124–1134. https://doi.org/10.1016/J.FOODHYD.2007.06.004.

(18) Aleandri, S.; Jankovic, S.; Kuentz, M. Towards a Better Understanding of Solid Dispersions in Aqueous Environment by a Fluorescence Quenching Approach. *Int. J. Pharm.* **2018**, *550* (1–2), 130–139. https://doi.org/10.1016/j.ijpharm.2018.08.029.

(19) Lacoulonche, F.; Chauvet, A.; Masse, J. An Investigation of Flurbiprofen Polymorphism by Thermoanalytical and Spectroscopic Methods and a Study of Its Interactions with Poly-(Ethylene Glycol) 6000 by Differential Scanning Calorimetry and Modelling. *Int. J. Pharm.* **1997**, *153* (2), 167–179. https://doi.org/10.1016/S0378-5173(97)00102-6.

(20) Law, D.; Wang, W.; Schmitt, E. A.; Qiu, Y.; Krill, S. L.; Fort, J. J. Properties of Rapidly Dissolving Eutectic Mixtures of Poly(Ethylene Glycol) and Fenofibrate: The Eutectic Microstructure. *J. Pharm. Sci.* **2003**, *92* (3), 505–515. https://doi.org/10.1002/jps.10324.

(21) Chiou, W. L.; Riegelman, S. Pharmaceutical Applications of Solid Dispersion Systems. *J. Pharm. Sci.* **1971**, *60* (9), 1281–1302. https://doi.org/10.1002/jps.2600600902.

(22) Ditzinger, F.; Scherer, U.; Schönenberger, M.; Holm, R.; Kuentz, M. Modified Polymer Matrix in Pharmaceutical Hot Melt Extrusion by Molecular Interactions with a Carboxylic Coformer. *Mol. Pharm.* **2018**, *16* (1), 141–150.

(23) Cheng, L.; Li, T.; Dong, L.; Wang, X.; Huo, Q.; Wang, H.; Jiang, Z.; Shan, X.; Pan, W.; Yang, X. Design and Evaluation of Bilayer Pump Tablet of Flurbiprofen Solid Dispersion for Zero-Order Controlled Delivery. *J. Pharm. Sci.* **2018**, *107* (5), 1434–1442.

(24) Furst, E. M.; Squires, T. M. *Microrheology*, 1st ed.; OUP Oxford, Ed.; OUP Oxford, 2017.

(25) Constantin, D.; Knaebel, A.; Bellour, M.; Padding, J. T.; Boek, E. S. Microrheology of Giant-Micelle Solutions. **2002**.

(26) Bellour, M.; Skouri, M.; Munch, J.-P.; Hébraud, P. Brownian Motion of Particles Embedded in a Solution of Giant Micelles. *Eur. Phys. J. E* **2002**, *8* (4), 431–436.

https://doi.org/10.1140/epje/i2002-10026-0.

(27) Niederquell, A.; Machado, A. H. E. E.; Kuentz, M. A Diffusing Wave Spectroscopy Study of Pharmaceutical Emulsions for Physical Stability Assessment. *Int. J. Pharm.* **2017**, *530* (1–2), 213–223. https://doi.org/10.1016/j.ijpharm.2017.07.038.

(28) Niederquell, A.; Dujovny, G.; Probst, S. E.; Kuentz, M. A Relative Permittivity Approach for Fast Drug Solubility Screening of Solvents and Excipients in Lipid-Based Delivery. *J. Pharm. Sci.* **2019**, *108* (10), 3457–3460. https://doi.org/10.1016/j.xphs.2019.06.014.

(29) Law, S. L.; Lo, W. Y.; Lin, F. M.; Chaing, C. H. Dissolution and Absorption of Nifedipine in Polyethylene Glycol Solid Dispersion Containing Phosphatidylcholine. *Int. J. Pharm.* **1992**, *84* (2), 161–166. https://doi.org/10.1016/0378-5173(92)90056-8.

(30) Lacoulonche, F.; Chauvet, A.; Masse, J.; Egea, M. A.; Garcia, M. L. An Investigation of FB Interactions with Poly(Ethylene Glycol) 6000, Poly(Ethylene Glycol) 4000, and Poly-ε-Caprolactone by Thermoanalytical and Spectroscopic Methods and Modeling. *J. Pharm. Sci.* **1998**, *87* (5), 543–551. https://doi.org/10.1021/js970443+.

(31) Lauritzen, J. I.; Hoffman, J. D. Formation of Polymer Crystals with Folded Chains from Dilute Solution. *J. Chem. Phys.* **1959**, *31* (6), 1680–1681. https://doi.org/10.1063/1.1730678.

(32) Tang, X.; Chen, W.; Li, L. The Tough Journey of Polymer Crystallization: Battling with Chain Flexibility and Connectivity. *Macromolecules* **2019**, *52* (10), 3575–3591. https://doi.org/10.1021/acs.macromol.8b02725.

(33) He, P.; Yu, W.; Zhou, C. Agglomeration of Crystals during Crystallization of Semicrystalline Polymers: A Suspension-Based Rheological Study. *Macromolecules* **2019**, *52* (3), 1042–1054. https://doi.org/10.1021/acs.macromol.8b02452.

(34) Ballard, M. J.; Buscall, R.; Waite, F. A. The Theory of Shear-Thickening Polymer Solutions. *Polymer (Guildf).* **1988**, *29* (7), 1287–1293. https://doi.org/10.1016/0032-3861(88)90058-4.

(35) MacMillan*, S. D.; Roberts, K. J.; Rossi, A.; And, M. A. W.; Polgreen, M. C.; Smith, I. H. In Situ Small Angle X-Ray Scattering (SAXS) Studies of Polymorphism with the Associated Crystallization of Cocoa Butter Fat Using Shearing Conditions. **2002**. https://doi.org/10.1021/CG0155649.

(36) Strobl, G. R.; IUCr. Determination of the Lamellar Structure of Partially Crystalline Polymers by Direct Analysis of Their Small-Angle X-Ray Scattering Curves. *J. Appl. Crystallogr.* **1973**, *6* (5), 365–370. https://doi.org/10.1107/S0021889873008897.